Propagation in Ferrite Loaded Coaxial Line

Propagation in Ferrite Loaded Coaxial Line*

By

Seiji KUNIYOSHI**

1. Introduction

This paper presents the results of an investigation of electromagnetic wave propagation in a coaxial line completely filled with gyromagnetic medium with longitudinal magnetization.

Theoretical derivations are based on Epstein's statement.[1] The external magnetic field dependence upon the propagation constant is formulated as a compatibility equation, whose solution gives us the propagation constant as a function of the anisotropy of the ferrite material.

Experimental investigations stand on the measurements of three quantities; a dielectric constant, an insertion loss and a propagation constant. The standing wave pattern along the slotted ferrite filled coaxial line was obtained by a movable detector along the coaxial line for the measurement of the propagation constant.

Experimental results show a good agreement with the results obtained from the calculations of the transcendental equation for the determination of the propagation constant.

2. Transcendental Equation and its Calculation for the Propagation Constant

Following Epstein's statement,[1] the transcendental equation for the determination of the permissible propagation constant in the coaxial line is derived as a function of an anisotropy of the ferrite material. The same assumptions, which were treated in the former paper,[2] are adopted in the process of the derivation of the basic equation.

The basic expression for the electric field is derived in the tensor form.

$$E=(S_E)\cdot\nabla\cdot\Psi \qquad \text{where} \quad (S_E)=\begin{vmatrix} j\sigma & \tau & 0 \\ -\tau & j\sigma & 0 \\ 0 & 0 & -j\sigma k^2/\Gamma^2 \end{vmatrix} \tag{1}$$

where Ψ is a wave function which is obtained as a solution of the wave equation, and the parameters in the tensor is abbreviated as follows.

$$\begin{aligned} k_1&=[(\varepsilon\omega^2-M_1\Gamma^2)\cdot(M_1+M_3)+K^2\Gamma^2\pm f]/2M_1M_3 \\ f&=[(M_1-M_3)\cdot(\varepsilon\omega^2-M_1\Gamma^2)^2+2(M_1+M_3)\cdot(\varepsilon\omega^2-M_1\Gamma^2)K^2\Gamma^2+K^2(K^2+4M_1M_3)\Gamma^4]^{1/2} \\ \tau_{\frac{1}{2}}&=M_1(k_{\frac{1}{2}}^2+\Gamma^2)-\varepsilon\omega^2, \qquad \sigma=K\Gamma^2 \end{aligned} \tag{2}$$

which can be expressed in terms of the propagation constant Γ and the anisotropy μ_a in the gyromagnetic medium.

$$\begin{aligned} k_{\frac{1}{2}}&=\omega\sqrt{\varepsilon\mu_1}\,[1-\Gamma_r^2-\mu_a^2/2\pm\mu_a\sqrt{(\mu_a/2)^2+\Gamma_r^2}\,]^{1/2} \\ \tau_{\frac{1}{2}}&=\omega^2\varepsilon\mu_a[\mu_a/2\pm\sqrt{(\mu_a/2)^2+\Gamma_r^2}\,]/(1-\mu_a^2) \\ \sigma&=\omega^2\mu_a/(1-\mu_a^2) \end{aligned} \tag{3}$$

* This paper is in part based on the thesis presented by the author for the partial requirement of the degree of master of science to the faculty of the graduate school of Northwestern University.

** Agriculture, Home Economics and Engineering Division, University of the Ryukyus.

where $\Gamma_r=\Gamma/\omega\sqrt{\varepsilon\mu_1}$ is the propagation constant normalized by $\omega\sqrt{\varepsilon\mu_1}$ which is the propagation constant of the plane wave propagation in unbounded isotropic medium with constants ε and μ_1.

In order to satisfy the scalar wave equation for the coaxial cylindrical line system, the wave function in Eq. (1) is represented as the sum of the Bessel and the Neumann function.

$$\Psi=[J_n(k_1r)+N_n(k_1r)]\cdot\exp\cdot j(n\varphi+\Gamma z) \tag{4}$$

Hence all the components of the electric field are obtained by substituting Eq. (9) into Eq. (6).

$$\begin{aligned}
&E_{1\varphi}(k_1r)=k_1\tau_1J_n(k_1r)-n(\tau_1+\sigma)J_n(k_1r)/r=-k_1\tau_1J_n(k_1r)-n\sigma J_n(k_1r)/r\\
&E_{1\varphi}(k_1r)=k_1\tau_1N_n(k_1r)-n(\tau_1+\sigma)N_n(k_1r)/r=-k_1\tau_1N_n(k_1r)-n\sigma N_n(k_1r)/r\\
&E_{1z}(k_1r)=\mu_ak_1^2J_n(k_1r)/\Gamma^2\\
&E_{1z}(k_1r)=\mu_ak_1^2N_n(k_1r)/\Gamma^2
\end{aligned} \tag{5}$$

Since the two values of k in Eq. (8) are available, the compete expressions of E_φ and E_z become.

$$\begin{aligned}
E_\varphi&=A_1E_{1\varphi}+A_2E_{2\varphi}+A_1E_{1\varphi}+A_2E_{2\varphi}\\
E_z&=A_1E_{1z}+A_2E_{2z}+A_1E_{1z}+A_2E_{2z}
\end{aligned} \tag{6}$$

For the convenience of the calculation, we assume that the coaxial line has the outer radius $r_0=1$ and the inner radius $r_i=R$. The boundary conditions at the walls of the inner and the outer cylinder are

$$E_\varphi=E_z=0 \quad \text{at} \quad r=1 \quad \text{and} \quad r=R \tag{7}$$

Substitution of Eq. (11) into Eq. (12) leads to a system of four simultaneous equations which are linear and homogeneous in the four A and they are compatible when

$$\begin{vmatrix}
E_{1\varphi}(1) & E_{2\varphi}(1) & E_{1\varphi}(1) & E_{2\varphi}(1)\\
E_{1z}(1) & E_{2z}(1) & E_{1z}(1) & E_{2z}(1)\\
E_{1\varphi}(R) & E_{2\varphi}(R) & E_{1\varphi}(R) & E_{2\varphi}(R)\\
E_{1z}(R) & E_{2z}(R) & E_{1z}(R) & E_{2z}(R)
\end{vmatrix}=0 \tag{8}$$

This is the transendental equation for the determination of the permissible propagation constant Γ of the electric wave propagating in the coaxial waveguide completely filled with the gyromagnetic medium. This equation meets the practical difficulty to solve for the propagation constant as a function of the anisotropy. However we consider the case for $n=0$, which corresponds to the dominant electric mode propagating in the gyromagnetic medium. By substituting Eq. (5) into Eq. (8) for $n=0$, we obtain the equation.

$$\begin{vmatrix}
\tau_1J_1(k_1) & \tau_2J_1(k_2) & \tau_1N_1(k_1) & \tau_2N_1(k_2)\\
\tau_1J_1(k_1R) & \tau_2J_1(k_2R) & \tau_1N_1(k_1R) & \tau_2N_1(k_2R)\\
J_0(k_1) & J_0(k_2) & N_0(k_1) & N_0(k_2)\\
J_0(k_1R) & J_0(k_2R) & N_0(k_1R) & N_0(k_2R)
\end{vmatrix}=0 \tag{9}$$

Since k_1 and k_2 are functions of the normarized propagation constant Γ_r and the anisotropy μ_a, the permissible values of the propagation constant should be satisfied by the above equation (9) under the assumed values of the anisotropy μ_a. The numerical ealculation of the determinant of the Eq. (9) was done for the help of the digital electronics computer *IBM*-650. The following numerical values, which were obtained from the experiments, were adopted for the computation of the determinant.

$$f=1280\,\text{mc/s} \quad \varepsilon=14.5 \quad \mu_1=1 \quad R=0.4 \tag{10}$$

The numerical calculation of the determinant in Eq. (9) proceeds the following steps.

(1) Computation of τ_1 in Eq. (3) over the range $0<\mu_a<1.0$ and $0<\Gamma_r^2<1.1$.

(2) Computation of k_1 in Eq. (3) over the range $0<\mu_a<1.0$ and $0<\Gamma_r^2<1.1$.

(3) Computation of the absolute value of the determinant in Eq. (9) by substituting τ_1

and k_1, which we obtained in the step (1) and (2), into Eq. (9) over the range $0<\mu_a<1.0$, and $0<\Gamma_r^2<1.1$.

The result of the calculation is shown Fig. (1). The calculated values of the determinant in Eq. (9) were plotted against each value of the parameter μ_a.

The result shows that the calculated values of the determinant have several infinit points at certain values of the normarized propagation constant Γ_r^2 over the range for $0<\mu_a<1.0$. Since we calculate the absolute value of the determinant, the zero values for the determinant are probably close to the unbounded points which give us the values of the permissible nor-

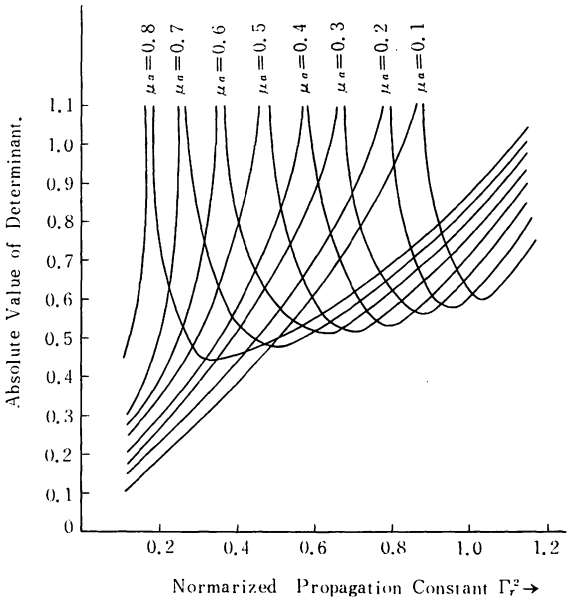

Fig. 1. Determinant vs. Propagation constant as a parameter of Anisotropy.

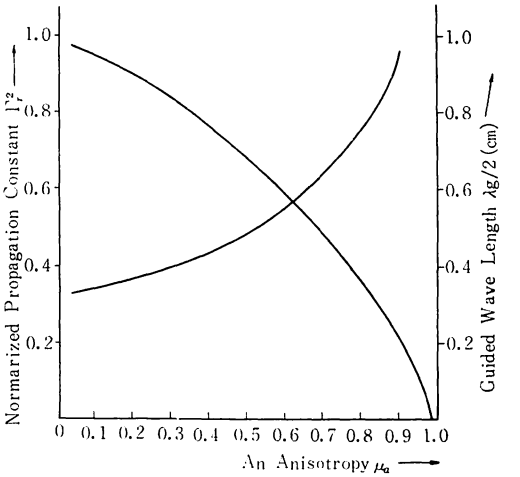

Fig. 2. Magnetic Field Dependence upon Propagation Constant and Guided Wave Length for Dominant Mode.

marized propagation constant Γ_r^2 which we are going to obtain. A plot of Γ_r^2 versus μ_a is shown in Fig. (2). Also the relationship between half wavelength $\lambda g/2$ and the anisotropy μ_a is shown in the same Figure. The result shows that the propagation constant behaves to decrease as the external applied magnetic field intensity increases which, as will be shown, follows the experimental results.

Since the propagation constant consists of the attenuation constant and the phase constant, and the attenuation constant is small enough to be neglected in comparison with the phase constant, the calculated value of Γ_r^2 indicates to be identical with the phase constant. As the result, the phase constant behaves to decrease as the external D. C. magnetic field increases.

3. Experimental Techniques for the Ferrite filled Coaxial Line

The several experimental attacks have been done for both thin ferrite and long ferrite, which is completely filled in coaxial line, on the basis of the measurements of three quantities, a dielectric constant of the ferrite, an insertion loss in the coaxial line filled with ferrite and a propagation constant of the electric wave propagating to the direction of the longitudinal magnetization.

(*1*) *Dielectric Constant*

Fig. (3) shows the whole apparatus used throughout the measurements of the dielectric constant of the ferrite. It consists of modulation square wave generator, signal generator, standing wavemeter, Ballantine vacuum tube voltmeter and the slotted coaxial line which is loaded with the ferrite TT414, manufactured by Grans. Tech. Inc. Assuming the dielectric constant of the ferrite $\varepsilon=14.5$, the ferrite was prepared by cutting a length $l=1.14$ (cm) which is approximately equal to a quarter wavelength at $f=1600$ mc/s. The voltage standing wave ratio and the guided wavelength were measured by the standing wavemeter by changing the frequency from the signal generator. The relationship between the reflection coefficient and the guided wavelength was plotted in Fig. (4). As Hippel[3] states, the maximum of the reflection coefficient occurs at old multiples of the quarter guided wavelength of the sample thickness, and minimums at the odd multiples of the half guided wavelength. Hence the

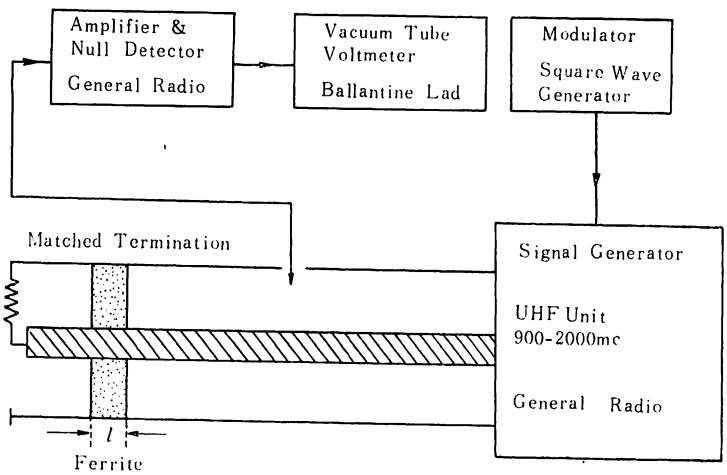

Fig. 3. Measurement of Dielectric Constant.

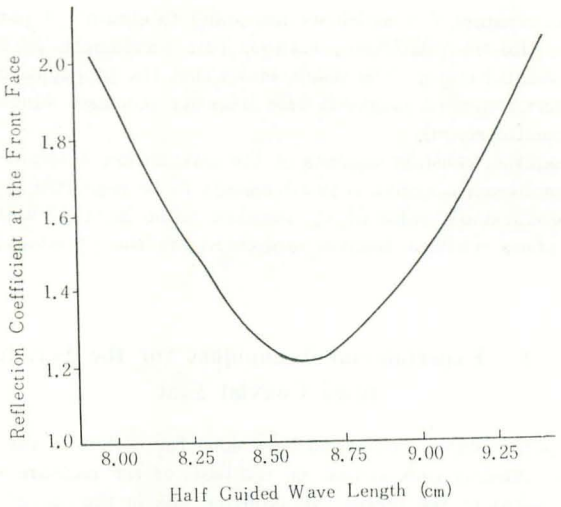

Fig. 4. Reflection Coefficient vs Guided Wavelength.

reflection coefficient should be minimum when the sample thickness l is equal to $\lambda g/2\sqrt{\varepsilon_f}$ where the dielectric constant of the ferrite is denoted by ε_f. From Fig. (4), we find that the minimum reflection coefficient ρ_0 occurs at the half wavelength $\lambda g/2=8.60$ (cm). Therefore the dielectric constant ε_f is obtained by $\varepsilon_f=(\lambda g\cdot \text{mini}/2l)^2=56.0$ where $\lambda g\cdot$mini denotes the guided wavelength at the minimum standing wave ratio and l is the sample thickness. Since the published value of ε_f and μ_f are 11.5 and 4.85 for the ferrite TT 414 respectively, the above observed value indicates that we are observing an initial permeability of the ferrite by $\varepsilon_f\cdot\mu_f=56.0$.

(2) *Insertion Loss*

The insertion loss, which comes from two factors that are (a) the attenuation loss due to the inserted material in the waveguide and (b) the transmission loss of the waveguide itself,

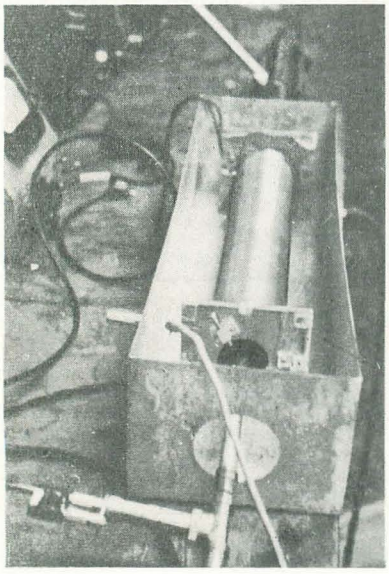

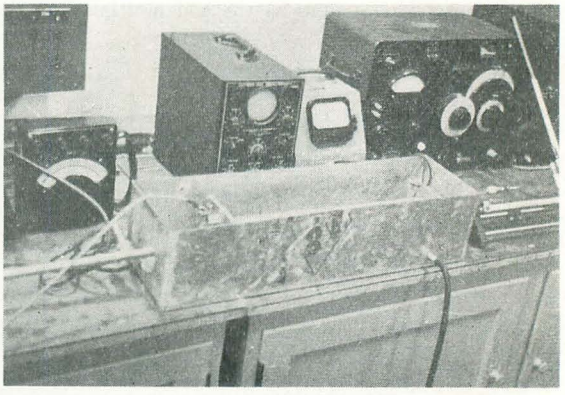

Fig. 5. Arrangement of the Entire Apparatus.

Fig. 6. External Field Coil and Colling Apparatus.

can be measured as the ratio of the input energy measured at the front of the ferrite to the output energy measured at the back of the ferrite. The energy, detected by the probe which is adjusted by an adjustable stub, was read by a vacuum tube voltmeter under the various values of the applied magnetic field. The effect of the magnetic field is shown in Fig. (8), which indicates the existance of the three different regions of the wave propagation.

I) *Small Magnetization* (below 120 gauss)

In this region the propagating electromagnetic wave see a unsaturated ferrite with a permeability of unit and with an ordinary dielectric constant ($\varepsilon=11.5$). Hence the wave propagates inside the ferrite with small insertion loss. Interface reflections cause some variation of the insertion loss as shown in Fig. (7).

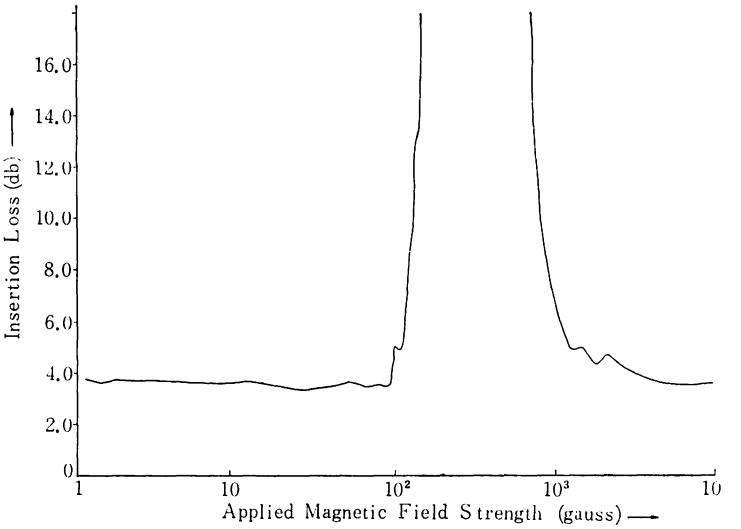

Fig. (7). Magnetic Field Dependence upon Insertion Loss.

II) *Middle Magnetization* (between 120 and 600 gauss)

As the applied magnetic field is gradually increased, the permeability of the ferrite approaches zero very rapidly as the permeability approaches zero, the wave length in the medium becomes longer and longer, and obviously before a zero permeability is reached, a phenomenon analogous to cutoff appears.

Therefore there should be a region when the permeability is close to zero where large reflections take place and very little power is propagated through a long slub of ferrite which fills the coaxial lines.

III) *Large Magnetization* (above 600 gauss)

The spin resonance appears in this region, which allows the wave to propagate, and the insertion loss decreases, which is identical with Hogan's statement.[4]

(3) *Propagation Constants*

As shown in the Fig. (8), the measurements of the propagation constant are based on the determination of the standing wave pattern in the ferrite filled coaxial line by moving a crystal detector along the slotted coaxial line under the various range of the magnetization of the ferrite.

As shown in Fig. (9), the slotted coaxial line is mounted with a crystal detector and an adjustable stub. The entire apparatus is inserted inside the magnetic field coil (radius is 5

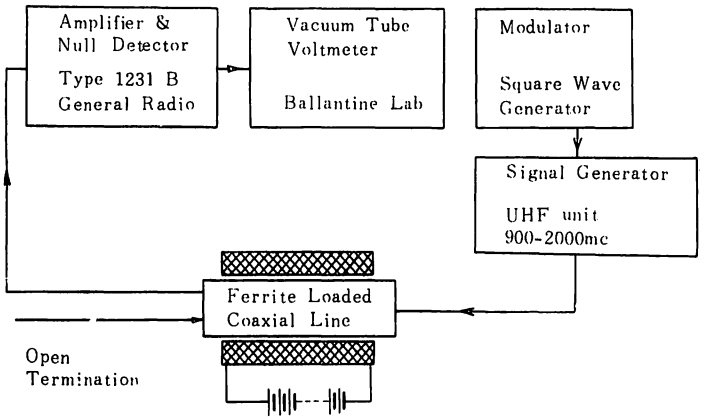

Fig. (8). Measurement of Propagation Constant.

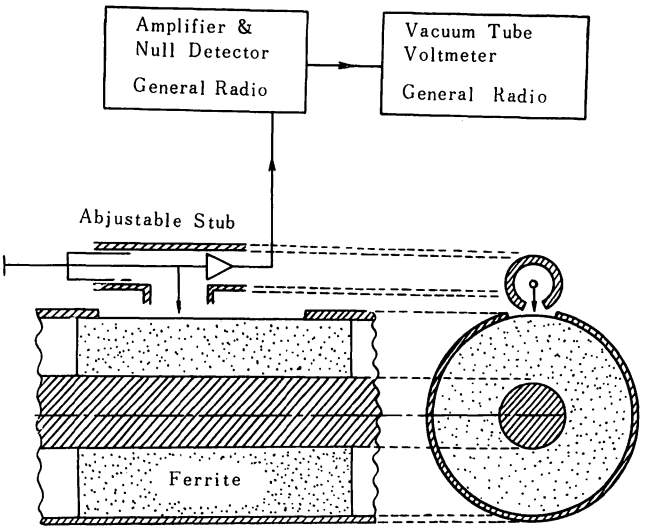

Fig. 9. Movable Detector.

cm) which is capable of a maximum current of 12 amperes. The detector is moved over the slotted line, containing the ferrite by a lead screw which extends to coutside the field coil.

A long ferrite cylinder (length 9.5 inches) was grounded to closely fit the slotted coaxial line. The pattern of the standing wave along the slotted coaxial line was observed in the oscilloscope by sliding the crystal mounted detector along the line and the detected energy was measured by Ballantine Vacuum Tube voltmeter.

The operating frequency $f=1280$ mc/s, was used throughout all the experiments. The magnetic field intensity in the field coil was measured by inserting the searching coil of the magnetic flux-meter (Kiro gauss-meter, Dyna Labs.) into the field coil, which was cooled down by ice and water when a large current was running in the coil. The signal generator was modulated by a 1,000 c/s. square wave. From the standing wave pattern, obtained in this experiment as shown in Fig. (10), the attenuation constant and the phase constant can be determined from the slope of the envelope and the guided wave length of the pattern.

a) *Attenuation Constant.*

Since the ratio at which the traveling wave decay incidates the attenuation constant, the standing wave pattern can be used to determine the attenuation constant of the travelling wave.

The result is shown in Table (1).

Table (1)

Field Strength (gauss)	Attenuation constant (neper/meter)	Field Strength (gauss)	Attenuation constant (neper/meter)
0.000	5.46	2.400	1.90
0.096	1.19	3.600	2.84
0.120	2.84	982.000	3.21
1.200	1.90	1200.000	0.05

The result indicates that in the region (I) the attenuation constant keeps unchanged and as the material becomes lossy, it causes domain wall rotation with the increasing magnetic field in the region (II) and the attenuation becomes large. Above 600 gauss in the region (III), the wave propagates again and the propagation constant becomes small as the material becomes low-lossy in the region (III).

b) *Phase Constant.*

The phase constant β can be determined from the measurement of the guided half wavelength of the standing wave pattern by use of the relationship $\beta=2\pi/\lambda g$. As shown in Fig. (10), the result indicates that, as the magnetic field increases in the region (I) the phase constant β decreases and the guided wave length increases which suggests the agreement with the result we obtained from the calculation in §2. Since no wave propagates in the cutoff region (II), the guided wavelength shows infinity and the phase constant becomes very small.

In the region (III) for the large magnetization, the electromagnetic wave propagates again and the phase constant β increases to keep a large value above $H_0=800$ gauss.

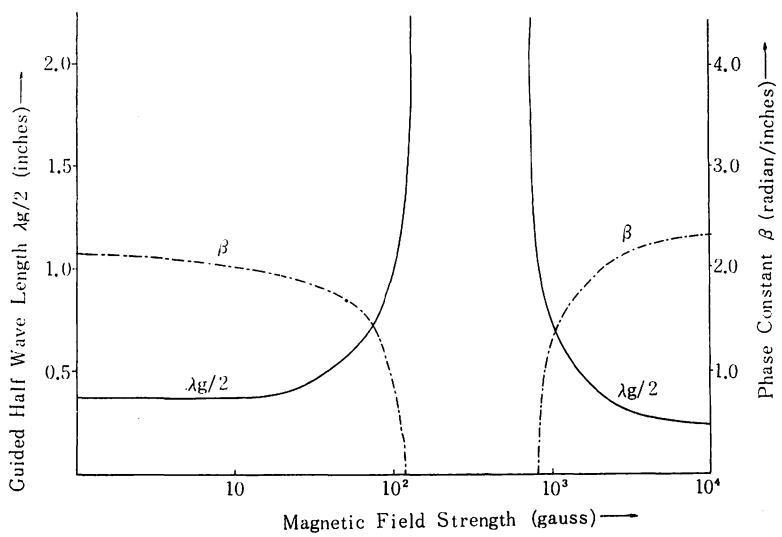

Fig. (10). Magnetic Field Dependence upon Guided Wave Length and Phase Constant.

4. Conclusion

The applied magnetic field dependence upon the propagation constant was studied from both experimental and theoretical points of view and results show the reasonable agreement that, as the magnetic field increases gradually, the wavelength becomes longer and longer until it reach up to the cutoff region. The measurement of the insertion loss reduces to the same result that there are three different regions of the wave propagation in the coaxial line, which can be classified by the degree of the magnetization of the ferrite. The results, obtained from the numerical calculation, indicate the first region of the wave propagation where the ferrite is magnetized below the domain wall motion.

References

1. Paul. S. Epstein: "Theory of Wave Propagation in Gyromagnetic Medium'.' Rev. of Mod. Phys. Vol. 28 No. 1 Jan. (1956).
2. Seiji Kuniyoshi: "Cutoff Frequencies of Circular Cylindrical Waveguides Containing Ferrites". (To be printed in the Science Bulletin at the Division of Agriculture, Home Economics & Engineering, Univ. of the Ryukyus. No. 8, 1961).
3. A. von Hippel, D. G. Jelatis, W. B. Westphal: "The Measurement of Dielectric Constant and Loss with Standing Waves in Coaxial Waveguide". N. D. R. C. Contract OE. Msr-191. Lab. for Insulation Res. MIT. April (1943).
4. C. L. Hogan: "Ferromagnetic Faraday Effect". Jan. (1953). Rev. Mod. Phys.

同軸線路に装荷されたフェライト内の電波伝播（摘要）

国　吉　清　治

軸方向に直流磁化をもつフェライトが，充鎮されている同軸線路内を伝播していく電磁界の伝播特性を示す超越方程式を導き，その計算値と同軸線路に沿って分布する定在波の波長測定より得られる実験値との比較検討を行った。

先づ理論的取扱いは，Epstein の導いたように，フェライトの透磁率を逆テンソルにとり，これに基ずいてフェライト内の電磁界の満足すべき基礎方程式 (1) から，その解として得られる同軸線路内の電磁界の表現式 (5) を得た。更にこの式に同軸線路の内壁及び外壁上での境界条件を適用して，線路内を伝播する電磁界の満足すべき特性式 (8) を導いた。これは各元素が第1種及び第2種の Bessel 函数で与えられる4行4列の行列式で，この式に含まれているパラメータ k 及び τ は，いづれも電磁界の伝播定数とフェライトの磁化の程度を示す非等方性係数 μ_a の函数として与えられる。この特性方程式の解は，IBM デジタル電子計算機 650 号を使用して数値計算され，伝播定数と非等方性係数との関係を示す結果が第2図に示された。尚，行列式の計算値は，第1図に示されるように，μ_a の或る値で無限大を示す結果が得られたが，これは行列式の絶対値を計算している事から，式 (9) の根は，その無限大を示す値に対する伝播定数がその解となると考えられる。計算結果は第2図に示されるように，フェライト磁化が進むにつれて，伝播定数は減少していく事を示す。

実験的基礎は，フェライトの誘電率，伝播定数及び挿入損失の測定に基づく。薄いフェライト板を同軸線路内に入れ，定在波測定法により得られる反射係数と管内波長との関係から，フェライトの誘電率 56 を得た。挿入損失の測定で，小直流磁化フェライトの場合には，伝播に履歴現象が見られ，遮断領域を越して再び伝播する領域のある事がわかった。伝播定数は探針をフェライトの充った線路に沿って移動させ，その定在波を探針位置の函数として測定し，その定在波の波形より減衰定数を直流磁場の値を変えて測定した。又定在波形から得られる管内波長より位相定数が計算され，これと直流磁場との関係は第10図に示され，伝播特性に遮断領域のある事がわかった。尚，第2章で数値計算されて得られた伝播定数は，この遮断領域の前の伝播領域に於ける伝播特性を表わす事が実験からわかった。